PHOTOSELECTION AND CIRCULAR DICHROISM IN THE PURPLE MEMBRANE

ROBIN E. GODFREY
Laboratorium für Biochemie, Eidgenössische Technische Hochschule, ETH-Zentrum, CH-8092 Zürich, Switzerland

ABSTRACT The transient dichroic ratio $D = \Delta A_{\parallel}/\Delta A_{\perp}$ has been measured in the visible absorption region of bacteriorhodopsin in purple membrane by a flash photolysis method. D is found to be wavelength independent throughout the visible absorption band, and reaches a maximum value of 2.75 ± 0.15 on reduction of the excitation intensity. This value is close to that expected for a single nondegenerate transition dipole moment and is incompatible with the strong exciton coupling model used to explain the visible circular dichroism (CD) spectrum of purple membrane. A time-dependent analysis of the exciton interaction and consideration of the coupling strength suggests an explanation of these observations. It is concluded that excitation interaction between retinals in purple membrane is of the weak or very weak type defined by Förster.

INTRODUCTION

The visible absorption spectrum of bacteriorhodopsin (BR) in the purple membrane of *Halobacterium halobium* is due to the protein-bound chromophore, retinal, which takes part in a photochemical cycle associated with the pumping of protons across the cell membrane (1, 2). The corresponding bisignate visible CD spectrum has been attributed to exciton interaction between adjacent chromophores (3, 4) within the trimeric groups of BR revealed by electron diffraction (5). These chromophore interactions would be expected to have some effect on the value of the polarization ratio, or dichroic ratio, for emission or absorption measurements, respectively, in a photoselection experiment (6), as the preferred orientation of molecules photoselected by a linearly polarized excitation will randomize to a certain extent as the excitation is transferred to neighboring chromophores having different orientations. Flash-induced transient linear dichroism studies on immobilized (in the millisecond time scale) BR have revealed, however, a high dichroic ratio (7, 8) little affected by energy transfer, and similar to the dichroic ratio of BR in the monomeric form in lipid vesicles before the decay due to protein rotation (9). A high degree of polarization has also been observed in the steady-state emission spectrum of BR (10).

In this paper we compare the dichroic ratio for purple membrane, measured as a function of wavelength, with the value predicted according to the formalism for strong coupling of excited chromophores in the BR trimer. We show that considering the evolution of the exciton system over time, and the strength of exciton coupling helps to reconcile the apparently contradictory CD and photoselection results.

EXPERIMENTAL

Excitation of BR at wavelengths within the broad visible absorption band (λ_{max} 568 nm) with a short-duration polarized light pulse results in anisotropic depopulation of the ground state and dichroism in the transient absorption spectrum, which persists for the duration of the photochemical cycle. The dichroic ratio D is defined by $D = \Delta A_{\parallel}/\Delta A_{\perp}$, where $\Delta A_{\parallel}$ and $\Delta A_{\perp}$ are the transient absorption changes at a fixed wavelength, polarized parallel and perpendicular to the polarization of the exciting light pulse, respectively.

Purple membrane was isolated from *H. halobium* according to published procedures (11), and measurements were carried out at 25°C on an aqueous suspension of light-adapted membrane of optical density about 1.0 (570 nm, 1-cm path length). The dichroic ratio for BR immobilized in purple membrane was determined using the flash photolysis apparatus described in reference 12 and outlined in the figure. We digitized the transient intensity changes parallel and perpendicular to the polarization of the exciting light pulse, and averaged up to 64 signals for improved signal-to-noise ratio. The averaged intensity changes were transferred to a desk-top computer, where the dichroic ratio was calculated and displayed on a curve plotter. A dead time of 20 μs was used between the laser excitation pulse (2-μs duration) and data collection to minimize the effect of scattered laser light, and the instrumental bandwidth was 1 MHz. An excitation wavelength of 540 nm was used and the measuring bandwidth maintained at <4 nm.

The inset in Fig. 1 shows a typical plot of D against time for a measuring wavelength of 570 nm and a laser-flash intensity such that ~8% of chromophores were excited into the photochemical cycle. D is virtually constant between 20 μs and 500 μs, though a small rise, approximately equal to the experimental uncertainty, is noticeable. In all cases, D is constant up to at least 1 ms, showing that the protein is immobilized on this time scale. As expected (12, 13) D was found to be dependent on the percentage of chromophores excited, and hence on the laser intensity. Table 1 shows the value of D (extrapolated back over 20 μs to zero time) as a function of the percentage of chromophores excited. At the lowest laser excitation used (4% chromophore excitation), D reached

Dr. Godfrey's present address is Photophysics Research, Ltd., London W1X 3HA, England.

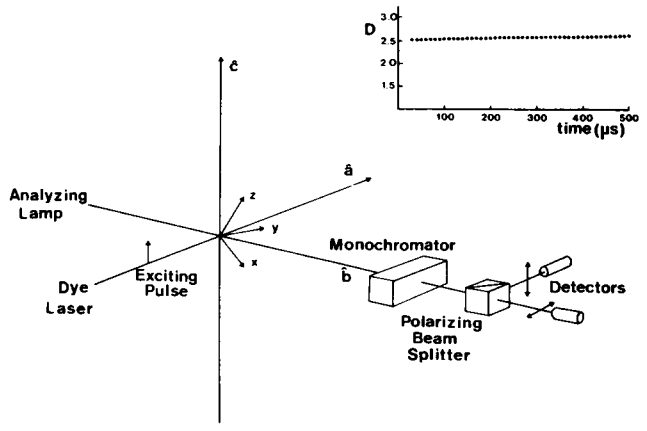

FIGURE 1 Schematic diagram of apparatus used to measure the dichroic ratio. x, y, z are the molecule-fixed axes, $\hat{\mathbf{a}}$, $\hat{\mathbf{b}}$, $\hat{\mathbf{c}}$ are the laboratory coordinates defining the excitation and measuring polarization. *Inset:* typical plot of D vs. time for purple membrane: 8% chromophore excitation, average of 64 signals, measuring wavelength 570 nm.

a maximum value of 2.75 ± 0.15. This may be compared with the value of 2.96 ± 0.06 reported by Ikegami and co-workers (8) on exciting only 1% of chromophores. The absolute value of D also depends on light scattering and alignment of the apparatus. For comparison, eosin immobilized in a polymer block gave similar dichroic ratios at comparable excitation intensities to purple membrane (12).

Table I also shows the value of D at various wavelengths together with the percentage excitation in each case. Within experimental error, D is seen to be independent of wavelength throughout the visible absorption band. The variation in chromophore excitation from ~4.5 to 8.5% would be expected to cause a variation in D by a factor of only 1.03 (Dr. S. Kawato, personal communication). Similar results were obtained using an excitation wavelength of 590 nm. The wavelength independence of D is consistent with the results of static linear dichroism measurements of oriented purple membrane (14).

TABLE I

Wavelength	Chromophore excitation*	D‡
nm	%	
570	4.0	2.75
570	5.5	2.55
570	8.0	2.50
570	9.0	2.45
570	14.0	2.20
570	15.0	2.15
570	16.5	2.15
570	17.5	2.10
570	19.5	2.05
570	27.0	1.90
520	5.5	2.60
530	6.0	2.60
540	6.0	2.60
550	8.5	2.55
560	6.5	2.60
580	7.0	2.60
590	8.5	2.50
600	4.5	2.70
610	7.5	2.60
620	7.5	2.60
630	7.5	2.55

*Experimental uncertainty ± 0.5%.
‡Extrapolated to time zero, experimental uncertainty ±0.15.

EXCITON COUPLING AND PHOTOSELECTION

Interaction between the transition dipole moments of a trimeric system lifts the degeneracy of the monomer excited-state energy levels, resulting in a single nondegenerate, ψ_+ and degenerate pair $\psi_-^{1,2}$ of excited stationary states, separated by $3V$, where V is the interaction energy between the transition dipole moments (15). Transitions to these three exciton states are mutually orthogonal, the doubly degenerate pair polarized perpendicular to each other and to the C_3 axis, which is normal to the membrane plane in the present case and along which the nondegenerate transition is polarized (15).

Evidence that the CD bands of purple membrane arise from transition dipole-moment interactions is given by retinal reconstitution experiments on bleached purple membrane (3), CD studies on oriented purple membrane films (16), and from the good correlation between CD magnitudes and protein aggregation, both in the purple membrane (17) and in artificial lipid bilayer systems (18). Although the two theoretical exciton CD bands are of equal magnitude (but opposite sign), the corresponding dipole strengths depend on the orientation of individual monomer transition moments (4). Several determinations indicate that these lie about 20° out of the membrane plane (14, 19, 20). The ratio of in-plane to out-of-plane dipole strengths is given by the ratio (4) $\sin^2\gamma$: $\cos^2\gamma$, which is about 8.5 if γ, the angle between the membrane normal and the transition moment, is 71° (14). The probability of excitation into the upper or lower energy exciton states also depends to some extent on the wavelength, particularly if the states are separated by a large energy interval. The indications are, however, that the exciton splitting in purple membrane is small, so that the in-plane transition probabilities would dominate irrespective of wavelength.

Based on this steady-state model of strong exciton coupling, we now derive the dichroic ratios for two idealized cases of ground-state absorption depletion, involving degenerate and nondegenerate transitions, assuming that the long-lived photoproducts do not themselves absorb light at the same wavelength as the ground-state molecules.

Nondegenerate Transition

Fig. 1 illustrates the geometry of a photoselection experiment involving a nondegenerate transition in which $\hat{\mathbf{a}}$, $\hat{\mathbf{b}}$ and $\hat{\mathbf{c}}$ are unit vectors defining the laboratory-fixed axes. The orientation of the molecular-fixed coordinate system x, y, z is defined by the Euler angles, which we collectively call Ω (21), that rotate the molecular frame into the laboratory axes. The transition dipole moment is assumed

to lie along the x-axis and the excitation pulse is $\hat{\mathbf{c}}$-polarized and travels along the $\hat{\mathbf{a}}$-axis. After excitation, the absorption changes $\Delta A_{\parallel}$, parallel, and $\Delta A_{\perp}$, perpendicular, to the $\hat{\mathbf{c}}$-axis are measured along the direction $\hat{\mathbf{b}}$. $\Delta A_{\parallel}$ is taken to be proportional to the compound probability that a molecule orientated in the direction Ω would have absorbed light polarized parallel to $\hat{\mathbf{c}}$ if it had been in the ground state, multiplied by the probability that it is not in the ground state, having been excited by the initial pulse. Thus,

$$\Delta A_{\parallel} \propto [\tilde{\boldsymbol{\mu}}(\Omega) \cdot \hat{\mathbf{c}}]^2 [\tilde{\boldsymbol{\mu}}(\Omega) \cdot \hat{\mathbf{c}}]^2 P(t) \qquad (1)$$

and similarly for $\Delta A_{\perp}$

$$\Delta A_{\perp} \propto [\tilde{\boldsymbol{\mu}}(\Omega) \cdot \hat{\mathbf{c}}]^2 [\tilde{\boldsymbol{\mu}}(\Omega) \cdot \hat{\mathbf{a}}]^2 P(t) \qquad (2)$$

where $P(t)$ is the probability that the molecule remains in an excited or photochemically modified state during the measurement. Replacing the scalar products $\tilde{\boldsymbol{\mu}}(\Omega) \cdot \hat{\mathbf{c}}$ etc. by the direction cosines that rotate the molecular frame into the laboratory frame (21), and averaging over all directions in space we find that

$$\Delta A_{\parallel} \propto P(t) \frac{8}{5} \pi^2 |\tilde{\boldsymbol{\mu}}|^4 \quad \text{and} \quad \Delta A_{\perp} \propto P(t) \frac{8}{15} \pi^2 |\tilde{\boldsymbol{\mu}}|^4,$$

giving a dichroic ratio of 3. The polarization ratio for emission $I_{\parallel}/I_{\perp}$ involving two different transition moments has the same value provided the two moments are parallel (6).

Degenerate Transitions

Assuming that the two degenerate transition moments are polarized along the x and y molecular axes, the absorbance changes now depend on the probability that either the x or y molecular axes are favorably oriented with respect to the exciting and measuring polarizations. Thus

$$\Delta A_{\parallel} \propto \{[\tilde{\boldsymbol{\mu}}_x(\Omega) \cdot \hat{\mathbf{c}}]^2 + [\tilde{\boldsymbol{\mu}}_y(\Omega) \cdot \hat{\mathbf{c}}]^2\}\{[\tilde{\boldsymbol{\mu}}_x(\Omega) \cdot \hat{\mathbf{c}}]^2 + [\tilde{\boldsymbol{\mu}}_y(\Omega) \cdot \hat{\mathbf{c}}]^2\} P(t) \qquad (3)$$

and

$$\Delta A_{\perp} \propto \{[\tilde{\boldsymbol{\mu}}_x(\Omega) \cdot \hat{\mathbf{c}}]^2 + [\tilde{\boldsymbol{\mu}}_y(\Omega) \cdot \hat{\mathbf{c}}]^2\}\{[\tilde{\boldsymbol{\mu}}_x(\Omega) \cdot \hat{\mathbf{a}}]^2 + [\tilde{\boldsymbol{\mu}}_y(\Omega) \cdot \hat{\mathbf{a}}]^2\} P(t). \qquad (4)$$

As before, we average over all directions to give

$$\Delta A_{\parallel} \propto P(t) \frac{64}{15} \pi^2 |\tilde{\boldsymbol{\mu}}|^4 \quad \text{and} \quad \Delta A_{\perp} \propto P(t) \frac{48}{15} \pi^2 |\tilde{\boldsymbol{\mu}}|^4.$$

The dichroic ratio D is now $4/3$, again the same as for emission measurements (6). In the case of triple degeneracy, involving three mutually orthogonal transition moments, D reduces to 1, as there is no preferred orientation of photoselected molecules (6).

The exciton transitions involved in the steady-state description of the purple membrane CD spectrum correspond closely to the case of double degeneracy, since the major absorption intensity is associated with the in-plane moments. The dichroic ratio would then be expected to be $4/3$, this value being reduced if the out-of-plane transition is included. In practice, instrumental factors, depolarization due to light scattering and nonnegligible excitation of the sample tend to reduce the dichroic ratio from the idealized theoretical value (6, 13). However, the experimental D was found to be at least 2.75 ± 0.15, and similar to that for eosin immobilized in a polymer matrix, an example of a nondegenerate transition.

An explanation of the CD and photoselection results might be provided by dimer (22) rather than trimer coupling, if, for example, the three retinals were not structurally identical. Dimer exciton coupling would approximate to the nondegenerate case (see Nondegenerate Transition, above) if the in-plane transition was dominant. There is, however, no evidence to support this idea. For example, chemical analysis shows that all three retinals are in the all-*trans* conformation in the light-adapted membrane (23, 24). Further, the high value of D would only be compatible with a very minor contribution from the out-of-plane transition moments.

TIME-DEPENDENT EXCITON ANALYSIS AND COUPLING STRENGTH

The steady-state exciton model pictures the excitation as essentially delocalized over the entire trimeric system. A complementary time-dependent view is that the excitation transfers rapidly from one chromophore to another in a time that may be roughly estimated from the uncertainty principle, $\tau \sim \hbar/3V$ (25). A small interaction energy, V, implies an exciton migration rate which may be less than the rates of relaxation processes from the excited state. The dichroic ratio will depend on the competition between energy transfer and relaxation processes.

A general time-dependent wave function describing the evolution of the exciton-coupled system after excitation may be written as a sum of the complete set of steady-state functions (26).

$$\Psi(r, t) = \sum_k \langle \psi_k(r) \,|\, \Psi(r, t_0) \rangle \exp[-i\hat{\mathbf{H}}(t - t_0)/\hbar] \psi_k(r) \qquad (5)$$

where $\psi_k(r)$ are steady-state wave functions and $\hat{\mathbf{H}}$ is the complete system Hamiltonion. Assuming that at some initial time t_0, the chromophore c alone is excited, $\Psi(r, t_0)$ may be replaced by the product function $\phi_a \phi_b \phi'_c \exp(-i\hat{\mathbf{H}}t_0/\hbar)$ and the sum over k states reduced by consideration of the orthonormalization properties of the wave functions, giving for the time variation of the system,

$$\Psi(r, t) = a_a \phi'_a \phi_b \phi_c + a_b \phi_a \phi'_b \phi_c + a_c \phi_a \phi_b \phi'_c$$

where the coefficients a_a, a_b and a_c are time-dependent and ϕ_i ($i = a, b, c$) are monomer wave functions. The exciton motion among the chromophores is characterized by the time varying composition of $\Psi(r, t)$ in terms of the individually excited configurations, the probability that the excitation rests on one particular chromophore, i, being given by the square of the relevant coefficient $a_i^* a_i$ (25, 27).

Thus, e.g.,

$$a_c^* a_c = (4 \cos 3Vt/\hbar + 5)\ 1/9, \qquad (6)$$

showing that the probability that the monomer c is excited varies from a maximum of 1 at time 0 to its first minimum at time $\tau = h/6V$.

A wide range of values for V have been suggested in the literature. A curve-fitting analysis of the purple membrane spectra (4) gives $V = 209$ cm^{-1} corresponding to a calculated interchromophore distance of 15 Å, considerably less than the 26 Å revealed by a recent neutron diffraction study (20). Another estimate (27), 487 cm^{-1}, is derived on the assumption, probably incorrect (4), that the monomer absorption spectrum is given by that of the protein solubilized by detergent, and leads to a distance of only 10 Å between retinals. Hemenger (28) has proposed a value of 64 cm^{-1}, based on a moments analysis of the absorption and CD spectra, which should be independent of the effect of vibronic band shapes and monomer absorption wavelength. This value can accommodate an interchromophore distance of up to 20 Å. Consistent with this value is the analysis of absorption and CD measurements on thin films of purple membrane by Muccio and Cassim (16), which suggest that V is about 54 cm^{-1}. In view of the lack of wavelength dependence of the linear dichroism of purple membrane (14), which supports a small exciton splitting and the sounder analysis of Hemenger, we use $V = 60$ cm^{-1}, corresponding to an excitation transfer time of about 0.09 ps.

The results of picosecond absorption studies (29, 30) on the primary intermediates in the BR photochemical cycle following excitation have recently been analyzed by Ottolenghi and co-workers (2, 31). They conclude that the first detected intermediate, observed to rise within 1 ps after excitation (29) is a ground state entity J_{625}, absorbing at 625 nm and corresponding to an isomerized chromophore, which relaxes, accompanied by proton transfer, to a species absorbing at 610 nm, K_{610}. Ippen et al. (29), on the other hand, suggest that the 1-ps intermediate is associated with an induced protein conformational change due to electron redistribution in the chromophore. Whatever the true nature of the first intermediate in the BR photocycle, it is clear that the excited retinal can undergo rapid conversion to a species absorbing at a different energy to the normal ground state, thereby competing with resonance energy transfer. However, the 1-ps conversion time is considerably slower than the estimated exciton transfer time above, suggesting that the excitation may transfer between the three chromophores many times before photoconversion, randomizing the initial orientations of the photoselected molecules and reducing D to about $4/3$ (see above).

It is of course possible that formation of the first intermediate competing with energy transfer is not detectable at the present level of instrumentation. Further, the measured rise time is that from excitation to the appearance of a ground-state species (31) absorbing at a different energy to the 568 nm transition. A more direct comparison with τ would be the time of conversion of the initial excited electronic state of BR to a form inhibiting energy transfer. For example, torsional twisting about a bond in the excited state could occur in subpicosecond times.

A consideration of the strength of exciton coupling suggests an alternative means of accounting for the photoselection results. The exciton-coupling formalism outlined above is strictly applicable only to the case of strong exciton coupling, that is when V is much larger than w, the electronic bandwidth (25, 32). This condition implies that exciton transfer is very rapid compared with the time taken for the nuclei to relax to their equilibrium configuration after excitation. This vibrational relaxation time is characterized by the electronic bandwidth w. The converse condition, $2V \ll w$, defines the weak coupling regime (32), in which vibrational relaxation can occur faster than excitation transfer. In the strong coupling limit, all vibronic levels of one monomer are in resonance with those of the others. For weak coupling, however, resonance interaction is between individual vibronic levels only, and the interaction energy is reduced by a factor $\Sigma_{\eta\nu} S_{\eta\nu}^2$ the square of the Franck-Condon overlap integral summed over vibrational levels of excited η and unexcited ν vibronic states (33).

The individual vibronic exciton matrix elements may be written $v_{\eta\nu} = VS_{\eta\nu}^2$. Under weak coupling, then, the exciton transfer rate is reduced by a factor of the order $\Sigma_{\eta\nu} S_{\eta\nu}^2$ which may easily increase τ by an order of magnitude from the expected strong coupling value (25).

Many of the discussions of strong and weak coupling, with respect to spectral band shapes (34–36), assume that the individual vibronic bands are themselves infinitely sharp. However, the shortening of vibronic lifetimes, due to vibrational energy exchange among the many vibrational modes of a condensed system, broadens these bands so that their widths, $\Delta\epsilon$, are significant compared with w. The overlapping of many such bands, z say, such that $z\Delta\epsilon > w$, is one reason for the smooth, featureless absorption bands observed in solution spectra. Förster (25) considers this factor to be important in the discussion of exciton energy transfer in many systems, in particular for those in which $\Delta\epsilon \gg 2v_{\eta\nu}$, which defines the very weak coupling region. Following his argument, if the coupling strength is larger than for very weak coupling, i.e., if $v_{\eta\nu} \gg \Delta\epsilon/2$, and if the spectrum is smooth due to $z\,\Delta\epsilon > w$, then $2V \sim 2zv_{\eta\nu} \gg z\Delta\epsilon > w$, so that we are in the strong coupling

region. Conversely, if $2V \ll w$, then $2v_{\pi\pi} \ll \Delta\epsilon$, and the very weak coupling condition applies. For continuous spectra then, the weak coupling range reduces to zero, or is at most closely limited (25). The CD and absorption spectra of purple membrane are smooth and featureless, even at low temperatures (4) and V is certainly much less than the absorption bandwidth (~3,200 cm^{-1} at room temperature), implying that the Förster very weak condition applies and that previous analyses (4, 27) of the purple membrane CD in terms of strong exciton coupling are at best an oversimplification (29).

Under very weak coupling the excitation transfer rate is fundamentally altered from that for strong or weak coupling (25). In the latter cases the probability of exciton transfer shows a quadratic time dependence, at times so short that $3Vt/\hbar$ is small. However, vibrational energy exchange in the case of very weak coupling results in a linear initial variation of $a_c^* a_c$ with time.

The argument presented above assumes that vibrational energy exchange, a kind of collisional process, is the major factor determining vibronic bandwidths and hence the overall absorption band shape. An alternative to this lifetime broadening however, in particular for solid-state or aggregate spectra, is the inhomogeneous broadening resulting from differences in the local environments of chromophores (37, 38). This broadening is not based on an excited-state relaxation probability and would not inhibit efficient energy transfer within the trimer (25). However, the absorption bandwidths of the free chromophore (2) and the detergent solubilized BR (27) are similar to that of BR in the purple membrane, suggesting that lattice site inhomogeneities at least do not significantly affect the absorption bandwidth.

The very small apparent value of V supports at least the weak if not the very weak coupling description for purple membrane, and a greatly reduced exciton transfer rate from that associated with strong coupling. Because the relative rates of exciton transfer and photochemical conversion determine the probabilities of these competing pathways, it is apparent that the probability of preservation of the original transition moment direction is enhanced under the weaker coupling, so that the dichroic ratio would be expected to be greater than the value for a degenerate electronic transition. The question of finite excitation transfer time and photoselection was first raised by Ebrey et al. (4). Their discussion, however, was couched in terms of strong exciton coupling, involving very rapid exciton transfer and degenerate steady states, which, as we have shown, necessarily involve low dichroic ratios.

The strong exciton coupling model has often been used to rationalize inorganic (15) and organic (22, 39) CD spectra, particularly in assigning absolute configurations from the energy ordering and signs of the exciton bands. When the coupling strength is relatively small, however, it becomes important to allow for vibronic effects to ensure correct assignment of configuration (40). Hemenger (28) has shown that analysis of real CD spectra with finite bandwidths can at best lead to certain constraints on possible geometries, rather than exact chromophore orientations and separations. A theoretical treatment of exciton CD in the very weak coupling region does not appear to have been carried out. The increasing structural information available on the purple membrane might provide a good test for any such treatment.

I would like to thank Drs. M. P. Heyn and S. Kawato for helpful discussions, Dr. R. J. Cherry and Professor S. F. Mason for reading the manuscript, and Carmen Zugliani for expert technical assistance. I am grateful to the Swiss National Science Foundation for financial support.

Received for publication 21 January 1981 and in revised form 18 August 1981.

REFERENCES

1. Stoeckenius, W., R. H. Lozier, and R. A. Bogomolni. 1979. Bacteriorhodopsin and the purple membrane of Halobacteria. *Biochim. Biophys. Acta.* 505:215–278.
2. Ottolenghi, M. 1980. The photochemistry of the rhodopsins. *Adv. Photochem.* 12:97–200.
3. Bauer, P.-J., N. A. Dencher, and M. P. Heyn. 1976. Evidence for chromophore-chromophore interactions in the purple membrane from reconstitution experiments of the chromophore-free membrane. *Biophys. Struct. Mech.* 2:79–92.
4. Ebrey, T. G., B. Becher, B. Mao, P. Kilbride, and B. Honig. 1977. Exciton interactions and chromophore orientation in the purple membrane. *J. Mol. Biol.* 112:377–397.
5. Henderson, R., and P. N. T. Unwin. 1975. Three-dimensional model of purple membrane obtained by electron microscopy. *Nature (Lond.).* 257:28–32.
6. Albrecht, A. C. 1970. The method of photoselection and some recent applications. *Prog. React. Kinet.* 5:301–334.
7. Lozier, R. H., and W. Niederberger. 1977. The photochemical cycle of bacteriorhodopsin. *Fed. Proc.* 36:1805–1809.
8. Kouyama, T., Y. Kimura, K. Kinosita, Jr., and A. Ikegami. 1981. Immobility of the chromophore in bacteriorhodopsin. *FEBS (Fed. Eur. Biochem. Soc.) Lett.* 124:100–104.
9. Cherry, R. J., and R. E. Godfrey. 1981. Anisotropic rotation of bacteriorhodopsin in lipid membranes: comparison of theory with experiment. *Biophys. J.* 35:257–276.
10. Lewis, A., J. P. Spoonhower, and G. J. Perrault. 1976. Observation of light emission from a rhodopsin. *Nature (Lond.).* 260:675–678.
11. Oesterhelt, D., and W. Stoeckenius. 1974. Isolation of the cell membrane of *Halobacterium halobium* and its fractionation into red and purple membrane. *Methods Enzymol.* 31:667–678.
12. Cherry, R. J. 1978. Measurement of protein rotational diffusion in membranes by flash photolysis. *Methods Enzymol.* 54:47–61.
13. Kawato, S., and K. Kinosita, Jr. 1981. Time-dependent absorption anisotropy and rotational diffusion of proteins in membranes. *Biophys. J.* 35:277–296.
14. Heyn, M. P., R. J. Cherry, and U. Müller. 1977. Transient and linear dichroism studies on bacteriorhodopsin: determination of the orientation of the 568 nm all-*trans* retinal chromophore. *J. Mol. Biol.* 117:607–620.
15. Mason, S. F. 1968. The electronic spectra and optical activity of phenanthroline and dipyridyl metal complexes. *Inorg. Chim. Acta Rev.* 2:89–109.
16. Muccio, D. D., and J. Y. Cassim. 1979. Interpretation of the absorption and circular dichroic spectra of oriented purple membrane films. *Biophys. J.* 26:427–440.
17. Heyn, M. P., P.-J. Bauer, and N. A. Dencher. 1977. Protein-protein interactions in the purple membrane. *In* Biochemistry of

Membrane Transport. G. Semenza, and E. Carafoli, editors. Springer-Verlag, Berlin. 96–104.

18. Cherry, R. J., U. Müller, R. Henderson, and M. P. Heyn. 1978. Temperature-dependent aggregation of bacteriorhodopsin in dipalmitoyl and dimyristoylphosphatidylcholine vesicles. *J. Mol. Biol.* 121:283–298.
19. Bogomolni, R. A., S. B. Hwang, Y.-W. Tseng, G. I. King, and W. Stoeckenius. 1977. Orientation of the bacteriorhodopsin transition dipole. *Biophys. J.* 17:98a.
20. King, G. I., P. C. Mowery, W. Stoeckenius, H. L. Crespi, and B. P. Schoenborn. 1980. Location of the chromophore in bacteriorhodopsin. *Proc. Natl. Acad. Sci. U. S. A.* 77:4726–4730.
21. Albrecht, A. C., and W. T. Simpson. 1955. Spectroscopic study of Wurster's Blue and tetramethyl-*p*-phenylenediamine with assignments of electronic transitions. *J. Am. Chem. Soc.* 77:4454–4461.
22. Mason, S. F. 1979. General models for optical activity. *In* Optical Activity and Chiral Discrimination. S. F. Mason, editor. Reidel Publishing Co., Dordrecht, Holland. 1–24.
23. Pettai, M. J., A. P. Yudd, K. Nakanishi, R. Henselman, and W. Stoeckenius. 1977. Identification of retinal isomers isolated from bacteriorhodopsin. *Biochemistry.* 16:1955–1959.
24. Tsuda, M., M. Glaccum, B. Nelson, and T. G. Ebrey. 1980. Light isomerises the chromophore of bacteriorhodopsin. *Nature (Lond.).* 287:351–353.
25. Förster, Th. 1966. Delocalized excitation and excitation transfer, in Modern Quantum Chemistry. O. Sinanoglu, editor. Academic Press, Inc., New York. 93–137.
26. Schiff, L. I. 1968. Quantum Mechanics. McGraw-Hill Book Co., New York. 3rd edition. 53.
27. Kriebel, A. N., and A. C. Albrecht. 1976. Excitonic interaction among three chromophores: an application to the purple membrane of *Halobacterium halobium. J. Chem. Phys.* 65:4575–4583.
28. Hemenger, R. P. 1978. Analysis of aggregate optical spectra using moments. Application to the purple membrane of Halobacterium halobium. *J. Chem. Phys.* 69:2279–2285.
29. Ippen, E. P., C. V. Shank, A. Lewis, and M. A. Marcus. 1978. Subpicosecond spectroscopy of bacteriorhodopsin. *Science (Wash. D.C.).* 200:1279–1281.
30. Applebury, M. L., K. S. Peters, and P. M. Rentzepis. 1978. Primary intermediates in the photochemical cycle of bacteriorhodpsin. *Biophys. J.* 23:375–382.
31. Dinur, U., B. Honig, and M. Ottolenghi. 1981. Analysis of primary photochemical processes in bacteriorhodopsin. *Photochem. Photobiol.* 33:523–527.
32. Simpson, W. T., and D. L. Peterson. 1957. Coupling strength for resonance force transfer of electronic energy in Van der Waals solids. *J. Chem. Phys.* 26:588–593.
33. Förster, Th. 1960. Excitation Transfer in Comparative Effects of Radiation. M. Burton, J. S. Kirby-Smith, and J. L. Magee, editors. John Wiley & Sons, Inc., New York. 300–341.
34. Fulton, R. L., and M. Gouterman. 1964. Vibronic coupling II. Spectra of dimers. *J. Chem. Phys.* 41:2280–2286.
35. Perrin, M. H., and M. Gouterman. 1967. Vibronic coupling IV. Trimers and trigonal molecules. *J. Chem. Phys.* 46:1019–1028.
36. Weigang, O. E., Jr. 1965. Vibrational structuring in optical activity I. Vibronic coupling in the circular dichroism of dimers. *J. Chem. Phys.* 43:71–72.
37. Burland, D. M., and A. H. Zewail. 1979. Coherent processes in molecular crystals. *Adv. Chem. Phys.* 40:369–484.
38. Steinfeld, J. I. 1974. Molecules and Radiation. Harper & Row, New York. 23.
39. Harada, N., and K. Nakanishi. 1972. The exciton chirality method and its application to configurational and conformational studies of natural products. *Accounts Chem. Res.* 5:257–263.
40. Mason, S. F., B. J. Peart, and R. E. Waddell. 1973. Optical rotatory power of co-ordination compounds. Part XVI. Intermediate exciton coupling in the circular dichroism of trisbipyridyl complexes. *J. Chem. Soc. Dalton.* 944–949.